Supporting Information

Extensive Characterization of Choline Chloride and its Solid-Liquid Equilibrium with Water

Ana I. M. C. Lobo Ferreira[a], Sérgio M. Vilas-Boas[b,c], Rodrigo M. A. Silva[a], Mónia A. R. Martins[c], Dinis. O. Abranches[c], Paula C. R. Soares-Santos[c], Filipe A. Almeida. Paz[c], Olga Ferreira[b], Simão P. Pinho[b,*], Luís M. N. B. F. Santos[a,*], João A. P. Coutinho[c]

[a] CIQUP, Institute of Molecular Sciences (IMS)- Departamento de Química e Bioquímica, Faculdade de Ciências da Universidade do Porto, Rua Campo Alegre, 4169-007 Porto, Portugal

[b] Centro de Investigação de Montanha (CIMO), Instituto Politécnico de Bragança, Campus de Santa Apolónia, 5300-253 Bragança, Portugal

[c] CICECO − Aveiro Institute of Materials, Department of Chemistry, University of Aveiro, 3810-193 Aveiro, Portugal

*Corresponding authors: Simão P. Pinho, Luís M. N. B. F. Santos

Telephone: +351 273 303 086

Fax: +351 273 313 051

E-mail: spinho@ipb.pt, lbsantos@fc.up.pt

S1 X-ray powder diffraction

Table SI.1. X-ray data collection, crystal data and structure refinement details for the partially-hydrated ChCl structure at 358 K.

Data Collection	
Diffractometer	Empyrean PANalytical
Wavelength (Å)	Cu K$\alpha_{1,2}$ X-radiation
Temperature (K)	358
Geometry	Bragg-Brentano para-focusing optics
2θ range (º)	10.00 to 60.00
Unit Cell	
Formula	$C_5NO_{1.1}Cl$
Crystal system	Triclinic
Space group	*P*1
a / Å	5.82
b / Å	6.85
c / Å	8.62
α / º	55.71
β / º	56.64
γ / º	59.15
Volume/Å^3	226.72
Z	1
D_c/g cm^{-3}	1.86
Profile parameters	
Profile function	Fundamental parameters approach
Zero shift [2θº]	-0.031
Refinement details	
No. of independent reflections	136
No. of global refined parameters	108
R_p	1.58
R_{wp}	2.36
R_{exp}	0.89
Structure Reliability Factors	
R_{Bragg}	5.80

/

where $y_{i,o}$ and $y_{i,c}$ are the observed and calculated profile intensities, $I_{n,o}$ and $I_{n,c}$ the observed and calculated intensities, respectively. The summations run over *i* data points or *n* independent reflections. Statistical weights w_i are usually taken as $1/y_{i,o}$.

2 Differential Scanning Calorimetry

The temperatures and the standard molar enthalpies of transition ChCl were measured in a power compensation differential scanning calorimeter, PERKIN ELMER model Pyris Diamond DSC, using a heating rate of 0.0833 $K \cdot s^{-1}$ (5 $K \cdot min^{-1}$) and a constant flow of high purity (99.999%) gaseous nitrogen as protective gas. The samples were enclosed in hermetically sealed aluminum crucibles (50 μL). The temperature and heat flux scales calibrations of the device were performed by measuring the temperature and the enthalpy of fusion of some reference materials: benzoic acid, *o*-terphenyl, perylene, anthracene, naphthalene, 1,3,5-triphenylbenzene, diphenyl ether, 1,3-difluorobenzene, 1-heptanol and 1-hexanol. Sample loading into the crucibles was performed in a glove box under dry nitrogen. Thermal behavior of crystalline ChCl was evaluated following the same experimental procedure used in the calibration runs (Figure SI.1) and the experimental results are presented in Table SI.2. The temperatures of the phase transitions were determined as the onset temperatures of the peaks.

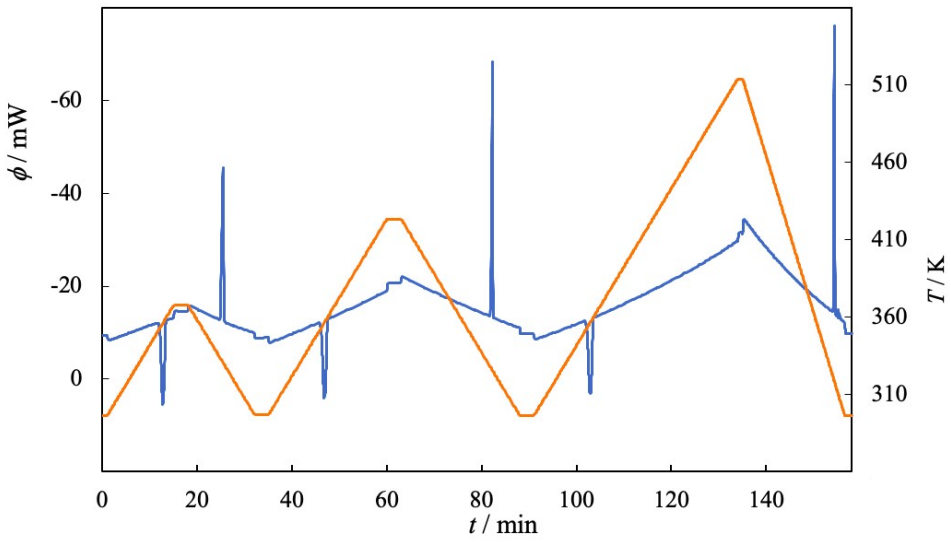

Figure SI.1. – Thermograms for ChCl heat flow *versus* time (Exp IV). Sample mass = 7.4055 mg.

Table SI.2. Experimental results (at p = 0.1 MPa) obtained for the study of the fusion equilibrium ChCl.

Exp.	m_{sample}/mg	$\Delta_{ss}H^{o}$exp / $J \cdot g^{-1}$	T_{ss} / K	$\Delta_{ss}H^{o}_{m}$ / $kJ \cdot mol^{-1}$	$\Delta_{ss}S^{o}_{m}$ / $J \cdot K^{-1} \cdot mol^{-1}$
I	4.6825	110.0	353.2	16.2	45.9
II	7.7654	110.0	352.1	16.2	46.0
III	7.8727	111.1	351.7	16.4	46.5
IV	7.4055	112.1	351.9	16.5	46.9

The kinetics of decomposition of ChCl was followed by DSC (Figure SI.2). Samples of pure ChCl were enclosed in aluminum crucibles with a hole in the lid. In Table SI.3 are presented the temperatures of decompositions, T_{dec}, at different scanning rates. In Figure SI.3 are given the experimental and estimated decomposition temperatures as function of scanning rates.

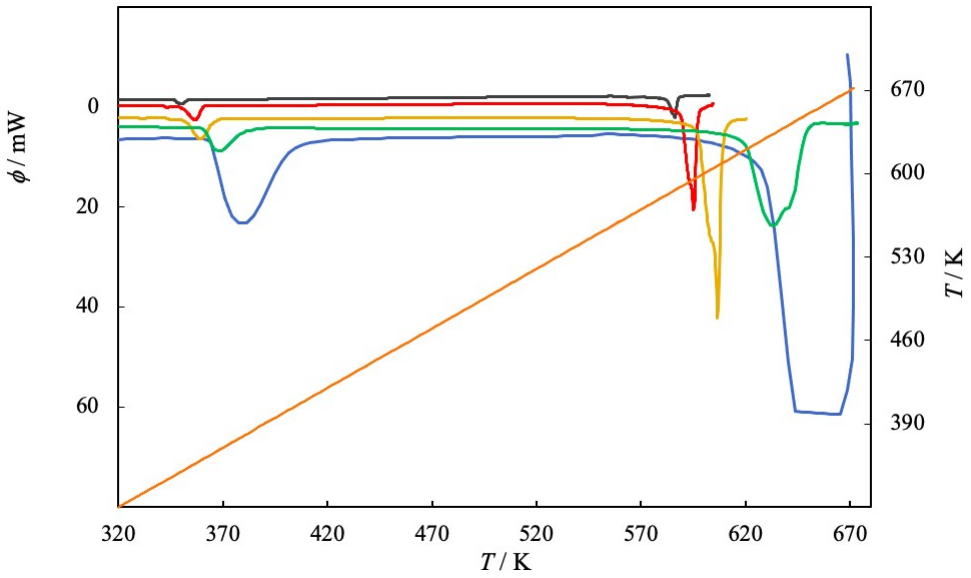

Figure SI.2. – Thermogram for ChCl, heat flow *versus* temperature until complete sample decomposition, at different scanning rates: — 5 K·min^{-1}; — 10 K·min^{-1}; — 20 K·min^{-1}; — 90 K·min^{-1}; — 200 K·min^{-1}.

Table SI.3. Decomposition temperatures, T_{dec}, of ChCl, measured by DSC, at different scanning rates.

Scanning rate/K·s^{-1}	T_{dec}/ K
0.0833 (5 K·min^{-1})	583 ± 5
0.1666 (10 K·min^{-1})	592 ± 5
0.3333 (20 K·min^{-1})	603 ± 5
1.5000 (90 K·min^{-1})	619 ± 5
3.3333 (200 K·min^{-1})	629 ± 5

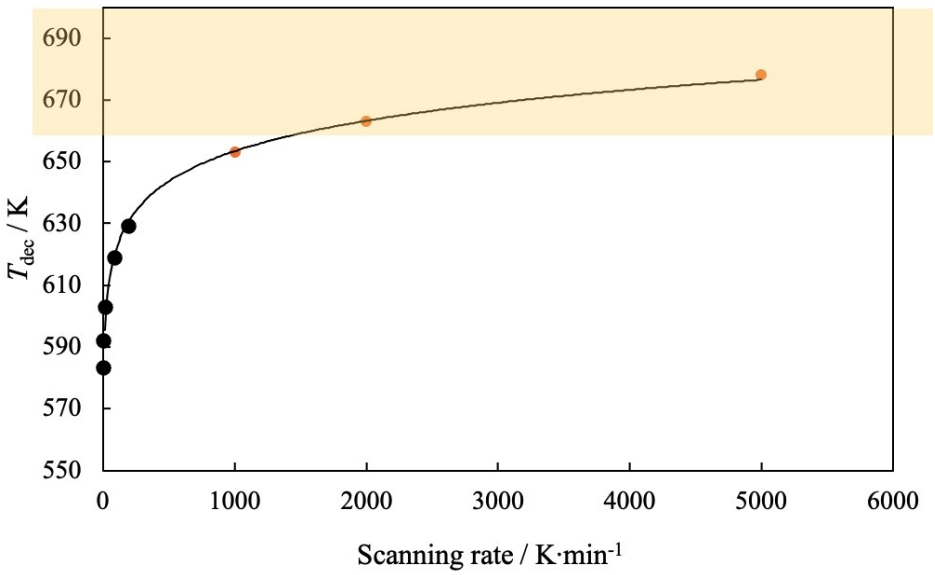

Figure SI.3. – Plot of decomposition temperature, $T_{dec,}$ *versus* scanning rate, of the DSC experiments of ChCl. ● – experimental T_{dec}; ● – estimated T_{dec}.

S3 High-precision heat capacity drop calorimeter at 298.15 K

The calorimeter was calibrated with sapphire (α-Al_2O_3 pellets, NIST-RM 720), based on a single drop temperature step procedure of $\Delta T = 10.00$ K, from the initial temperature $T_i = 303.15$ K to the final temperature $T_f = 293.15$ K, and using the respective standard molar heat capacity at 298.15 K reported in the literature, $C^{o}_{p,m}(\alpha\text{-}Al_2O_3) = 79.03 \pm 0.08$ J·K^{-1}·mol^{-1}.[1] The calibration constant of the calorimeter was found to be $\varepsilon = 6.6541 \pm 0.0206$ W·V^{-1}.

Benzoic acid (Calorimetric Standard NIST 39j) and hexafluorobenzene were used as test substances to evaluate the accuracy of the apparatus for the measurements of the heat capacities of solid and liquids compounds.[2–4] Additionally, the ionic liquid $[C_6C_1im][NTf_2]$ was used to check the accuracy of the calorimeter for the measurements of the heat capacities of ionic liquids: recommended value of $C^{o}_{p,m}([C_6C_1im][NTf_2], l, 298.15\ K) = 631.6 \pm 1.3$ J·K^{-1}·mol^{-1}.[5] The determined value achieved as the average of two independent experimental runs was $C^{o}_{p,m}([C_6C_1im][NTf_2], l, 298.15\ K) = 629.6 \pm 2.3$ J·K^{-1}·mol^{-1}, which is in excellent agreement with the literature recommend value.[4] The high-precision heat capacity drop calorimeter incorporates a fully automatic setup and data treatment, providing reliable high-quality heat capacity data for several compounds, liquid and solid samples.[1–3,6–9]

The detailed results of the heat capacities of the liquid binary mixtures of chloride choline and water (molar fraction $x_{ChCl} < 0.4$) at T=298.15 K, are presented in Table SI.4.

Table SI.4. Molar heat capacity values at T = 298.15 K for different mixtures of chloride choline and water. The calibration constant used to calculate the C_p values was the one derived from the sapphire [NBS, SRM 720, (α-Al_2O_3)] calibration, (6.6734 ± 0.0167 W·V^{-1}).

x_{ChCl}	M/g·mol^{-1}	m_{sample}/g	N_{drop}	$<T_{furnace}>$/K	$<T_{calorimeter}>$/K	$<T>$ /K	$C^{o}_{p,m}$/J·K^{-1}·mol^{-1}
0.060	24.0493	0.51750	33	303.32	293.18	298.25	80.7 ± 0.2
0.100	30.1634	0.51307	14	303.37	293.18	298.28	87.5 ± 0.3
0.150	36.2040	0.51766	86	303.33	293.18	298.26	95.6 ± 0.3
0.175	39.3839	0.50710	10	303.32	293.17	298.25	100.0 ± 0.5
0.197	41.9262	0.51696	23	303.30	293.18	298.24	103.5 ± 0.3
0.224	45.2582	0.49880	11	303.33	293.18	298.25	108.7 ± 0.3
0.248	48.2071	0.49649	78	303.37	293.18	298.28	113.1 ± 0.3
0.272	51.1140	0.53522	15	303.38	293.17	298.28	117.6 ± 0.3
0.299	54.3203	0.55606	56	303.31	293.18	298.25	121.8 ± 0.3
0.322	57.1297	0.56960	22	303.34	293.18	298.26	126.0 ± 0.3
0.356	61.2531	0.56628	52	303.34	293.17	298.26	132.5 ± 0.4

N_{drop} = number of drop experiments; $T_{furnace}$ = average temperature of the furnace; $T_{calorimeter}$ = average temperature of the calorimeter; the uncertainty reported is twice the standard deviation of the mean and the calibration uncertainty (ε) is included.

ΔT is calculated as $T_{furnace} - T_{calorimeter}$. Temperature sensors (Pt100) were calibrated by comparison with a certified platinum resistance thermometer, PTR100 (Fluke – Hart Scientific, Model 5626), traceable to the National Institute of Standards and Technology (NIST) based on the ITS-90 temperature scale, with an uncertainty smaller than 0.002 K. The temperatures is typically controlled to within ±($3\cdot10^{-3}$) K and measured with a resolution better than $1\cdot10^{-3}$ K and um uncertainty of $2\cdot10^{-2}$ K in the temperature range.

S4 Heat capacities measurements of ChCl by DSC and HC-DSC Calorimetry

The experimental heat capacities as a function of temperature were measured based on the step method procedure, using two different calorimeters. A heat conduction differential scanning type microcalorimeter (HC-DSC) SETARAM model (microDSC III) was used to measure the heat capacity in the temperature range of 283 to 333 K. A power compensation differential scanning calorimeter, PERKIN ELMER model (Pyris Diamond DSC) used to measure the heat capacity in the temperature range of 273 to 423 K.

The heat capacity results are presented in Tables SI.5 and SI.6. For the HC-DSC measurements, ΔT_{step} = 10 K, at 0.3 K·min^{-1}, $t_{isothermal}$ = 2400 s and for the DSC measurements, ΔT_{step} = 5 K, at 5 K·min^{-1}, $t_{isothermal}$ = 600 s. For the DSC measurements, the sample was kept in hermetically sealed 50 μL aluminum crucibles. In the HC-DSC runs, the sample was kept in a 1 cm^3 Hastelloy C276 cell, hermetically sealed with a *Viton* o-ring. The HC-DSC samples were weighted in a Mettler Toledo AT201 analytical balance, with a resolution of ± 0.00001 g. The DSC samples were weighted in a Mettler Toledo UMT5 micro balance, with a resolution of ± 0.0001 mg.

To test the fidelity of the DSC measurements, the heat capacity of the α crystalline phase was also evaluated. For this, in the first DSC experiment (Experiment 1 in Table SI.7) runs were made including a temperature interval where the choline chloride was in the α crystalline phase (between 280 and 340 K). In order to extend the temperature interval, a second experiment (Experiment 2 in Table SI.8) was done with choline chloride in the α crystalline phase, but at a lower temperature interval (between, 280 and 310 K). The same step temperature change (ΔT_{step}), scanning rate , and isothermal step duration ($t_{isothermal}$) was used in all DSC experiments. In both calorimeters the calibration was done using highly pure synthetic sapphire (α-Al_2O_3, NBS SRM-720)[1] using blanks experiments correction. A typical thermogram and the temperature program of one of the DSC runs is presented in Figure SI.4.

Table SI.5. Experimental heat capacity data obtained for each run through Tian-Calvet type differential scanning microcalorimetry (HC-DSC).

Experiment 1 (m_{sample} = 0.64132 g)

T / K	$C^{o}_{p,m}$ / J·K^{-1}·mol^{-1}	T / K	$C^{o}_{p,m}$ / J·K^{-1}·mol^{-1}	T / K	$C^{o}_{p,m}$ / J·K^{-1}·mol^{-1}
	Run 1		*Run 3*		*Run 5*
283.34	201.26	283.34	201.11	283.34	201.01
293.38	206.72	293.38	206.50	293.38	206.44
303.42	212.06	303.42	211.87	303.42	211.84
313.45	217.67	313.45	217.13	313.45	216.85
	Run 2	323.47	222.87	323.47	222.52
283.34	201.23	333.50	227.96	333.50	228.48
293.38	206.70		*Run 4*		*Run 6*
303.42	212.19	283.34	201.08	283.34	201.00
313.45	217.44	293.38	206.46	293.38	206.34
323.47	223.11	303.42	211.91	303.42	211.82
333.50	228.48	313.45	217.11	313.45	216.95
		323.47	222.64	323.47	222.49
		333.50	227.62	333.50	227.40

Experiment 2 (m_{sample} = 0.67630 g)

T / K	$C^{o}_{p,m}$ / J·K^{-1}·mol^{-1}	T / K	$C^{o}_{p,m}$ / J·K^{-1}·mol^{-1}	T / K	$C^{o}_{p,m}$ / J·K^{-1}·mol^{-1}
	Run 1		*Run 3*		*Run 5*
283.34	200.93	283.34	200.86	283.34	200.79
293.38	206.34	293.38	206.26	293.38	206.16
303.42	211.29	303.42	211.23	303.42	211.17
313.45	216.45	313.45	216.43	313.45	216.24
323.47	222.11	323.47	221.99	323.47	221.76
333.50	227.59	333.50	227.30	333.50	227.14
	Run 2		*Run 4*		
283.34	200.85	283.34	200.67		
293.38	206.22	293.38	206.12		
303.42	211.17	303.42	211.00		
313.45	216.25	313.45	216.16		
323.47	221.76	323.47	221.71		
333.50	227.12	333.50	227.02		

Table SI.6. Experimental heat capacity data obtained for each run through differential scanning calorimetry (DSC).

Experiment 1 (m_{sample} = 12.8670 mg)

T / K	$C^{o}_{p,m}$ / J·K^{-1}·mol^{-1}
Run 1	
363.6	261.7
368.6	263.6
373.7	264.6
378.8	266.4
383.9	267.8
389.0	269.5
394.0	271.7
399.1	273.6
404.2	274.5
409.2	277.0
414.3	278.1
419.4	279.5
Run 2	
322.9	219.6
328.0	222.1
333.1	224.2
338.1	225.9
α to β transition	
368.6	264.0
373.7	265.0
378.8	268.2
383.9	269.2
389.0	270.8
394.0	270.9
399.1	271.9
404.2	273.9
409.2	275.7
414.3	276.9
419.4	277.6

T / K	$C^{o}_{p,m}$ / J·K^{-1}·mol^{-1}
Run 3	
322.9	219.5
328.0	221.9
333.1	224.1
338.1	225.0
α to β transition	
368.6	262.5
373.7	264.0
378.8	267.1
383.9	267.3
389.0	270.7
394.0	273.1
399.1	272.1
404.2	273.2
409.2	276.1
414.3	277.5
419.4	278.2
Run 4	
322.9	219.0
328.0	221.9
333.0	224.0
338.1	225.0
α to β transition	
368.6	261.9
373.7	263.4
378.8	265.5
383.9	266.5
388.9	269.8
394.0	272.6
399.1	273.4

T / K	$C^{o}_{p,m}$ / J·K^{-1}·mol^{-1}
404.2	274.8
409.2	275.4
414.3	278.4
419.4	279.8
Run 5	
322.9	219.0
327.9	221.5
333.0	224.0
338.1	224.9
α to β transition	
368.6	262.0
373.7	263.6
378.8	265.9
383.9	267.2
388.9	269.0
394.0	271.6
399.1	274.0
404.1	275.6
409.2	275.9
414.3	279.2
419.3	278.1

Experiment 2 (m_{sample} = 3.7922 mg)

T / K	$C_{p,m}^{o}$ / J·K^{-1}·mol^{-1}
	Run 1
282.9	205.1
287.9	207.1
292.9	208.5
297.9	211.9
303.0	214.9
308.0	215.1

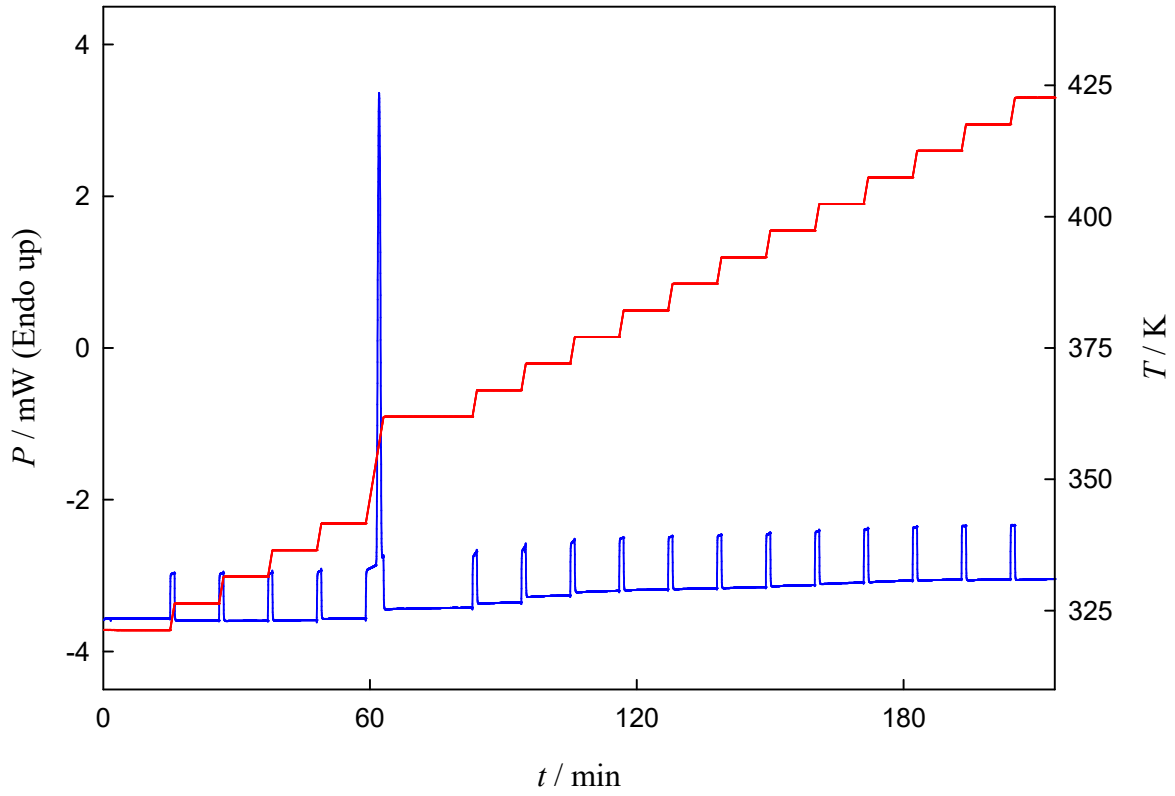

Figure SI.4. Thermogram (blue) and temperature program (red) of one of the ChCl scans for the determination of heat capacity through the isothermal step method with DSC (Experiment 1).

S5 Sample preparation

Binary mixtures of chloride choline and water [ChCl + H_2O] of approximately 2 g with different compositions were prepared gravimetrically using an analytical balance, Mettler Toledo, model AG245, with a mass resolution of ± 0.01 mg. All mixtures were prepared in a glove box under nitrogen atmosphere and kept in sealed glass bottles under nitrogen to avoid contamination. The mixtures of different composition (molar fraction between 0.0 and 1.0 in 0.1 mol fraction steps, and whenever was necessary additional binary mixtures were prepared in order to increase the resolution of the phase diagrams or heat capacities measurements) were heated (≈ 353 K), mixed and kept for 72 h in order to obtain a homogeneous solution. The overall uncertainty of the experimental mole fraction was estimated to be approximately ± 1×10^{-3}. Sample handling and preparation for the calorimetric measurements was always performed in a glove box (Captair pyramid 2200) under dry nitrogen atmosphere.

S6 ChCl + H_2O solid-liquid phase diagram

For the study of the solid-liquid equilibrium of the binary mixtures of ChCl + H_2O the following thermal procedure was done: first an isothermal step of 1 min at 298 K, followed by a heating step until 368 K and another isothermal step of 1 min. After this isothermal step the sample was cooled using scanning rate of 10 K·min^{-1} until 178 K and it was done another isothermal step of 5 min; a heating step of 5 K·min^{-1} was performed until 200 K, with the annealing of the sample during 20 min at 200 K. This step was followed by another scanning step at 10 K·min^{-1} until 178 K, followed by another isothermal of 10 min. The sample was now heated at 5 K·min^{-1} until 368 K followed by an isothermal step of 1 min. The thermograms for the chloride choline and ChCl + H_2O mixtures at different compositions are presented in Figure SI.5. A detailed plot of the solid-solid transition of ChCl for pure choline chloride and binary mixtures of ChCl + H_2O $\boldsymbol{x}_{ChCl} = 0.9$ and $\boldsymbol{x}_{ChCl} = 0.8$) is presented in Figure SI.6. The eutectic temperatures, $T_{eutectic}$, solid-solid transition temperatures, T_{ss}, melting temperatures, $T_{melting}$, for the different compositions (molar fraction of ChCl, $\boldsymbol{x}_{ChCl}$) of the binary mixtures ChCl + H_2O are given in Table SI.7.

Table SI.7. Different compositions (molar fraction of ChCl, x_{ChCl}) of the binary mixtures ChCl + H_2O, eutectic temperatures, $T_{eutectic}$, solid-solid transition temperatures, T_{ss}, melting temperatures, $T_{melting}$ and enthalpies of the solid-solid transitions.[a]

x_{ChCl}	m_{sample}/mg	$T_{eutectic}$ / K	T_{ss} / K	$T_{melting}$ / K	$\Delta_{ss}H^{o}_{m}$ / kJ·mol^{-1}
0.100	11.1213	203.1		249.0	
0.150	10.5021	204.5		230.2	
0.197	17.9522				
0.248	16.9899	200.2		238.4	
0.299	17.9518	204.5		264.8	
0.322	16.4122	204.5		275.3	
0.356	14.3214	204.6		292.1	
0.395	6.1127	204.7		304.2	
0.495	41.2497	204.7	341.0	337.0	0.8 ± 1.0
0.603	22.4682	204.7	340.5		3.7 ± 1.0
0.700	6.1908	204.2	340.0		8.4 ± 1.0
0.791	12.7892	204.2	340.0		10.1 ± 1.0
0.901	4.3247	204.5	340.0		14.0 ± 1.0

[a]The uncertainty of the experimental results σ (temperature) was estimated as ± 1.0 K for the temperature.

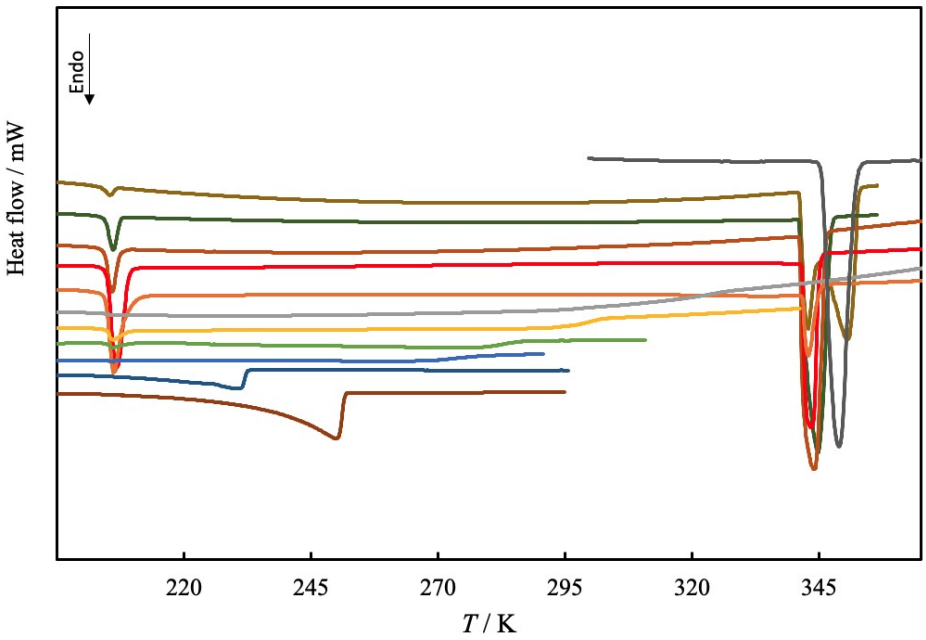

Figure SI.5. – Thermograms for the chloride choline (ChCl) and ChCl + H_2O mixtures at different compositions. — ChCl, — x_{ChCl} = 0.9, — x_{ChCl} = 0.8, — x_{ChCl} = 0.7, — x_{ChCl} = 0.6, — x_{ChCl} = 0.5, — x_{ChCl} = 0.4, — x_{ChCl} = 0.35, — x_{ChCl} = 0.325, — x_{ChCl} = 0.3, — x_{ChCl} = 0.15, — x_{ChCl} = 0.1.

The experimental results obtained by procedures 1 and 3 are compiled in Table SI.8, while in Figure SI.7 a comparison to the literature data is given.

Table SI.8. Melting temperatures in binary mixtures ChCl + H_2O at different water mole fraction $\boldsymbol{x}_{ChCl}$) and the solubility of ChCl in water at different temperatures.[a]

$\boldsymbol{x}_{ChCl}$	$T_{melting}$ / K	$\boldsymbol{x}_{ChCl}$	$T_{melting}$ / K	$\boldsymbol{x}_{ChCl}$	$T_{melting}$ / K
Procedure 1					
0.007	271.7	0.054	261.6	0.127	239.6
0.014	270.5	0.066	258.3	0.166	223.3
0.023	269.1	0.083	253.9	0.302	261.3
0.032	267.3	0.090	251.8	0.321	266.6
0.042	264.2	0.117	243.3	0.329	268.5
Procedure 3					
T / K	$\boldsymbol{x}_{ChCl}$	T / K	$\boldsymbol{x}_{ChCl}$	T / K	$\boldsymbol{x}_{ChCl}$
298.2[b]	0.364	323.2[b]	0.430	353.2	0.490
303.2[b]	0.376	328.2[b]	0.443	358.2	0.491
308.2[b]	0.389	333.2[b]	0.460	368.2	0.500
313.2[b]	0.403	338.2[b]	0.476	378.2	0.508
318.2[b]	0.416	343.2[b]	0.486	388.2	0.515

[a]The uncertainty of the experimental results σ (temperature) was estimated as ± 0.5 K for the temperature. b Reference [10].

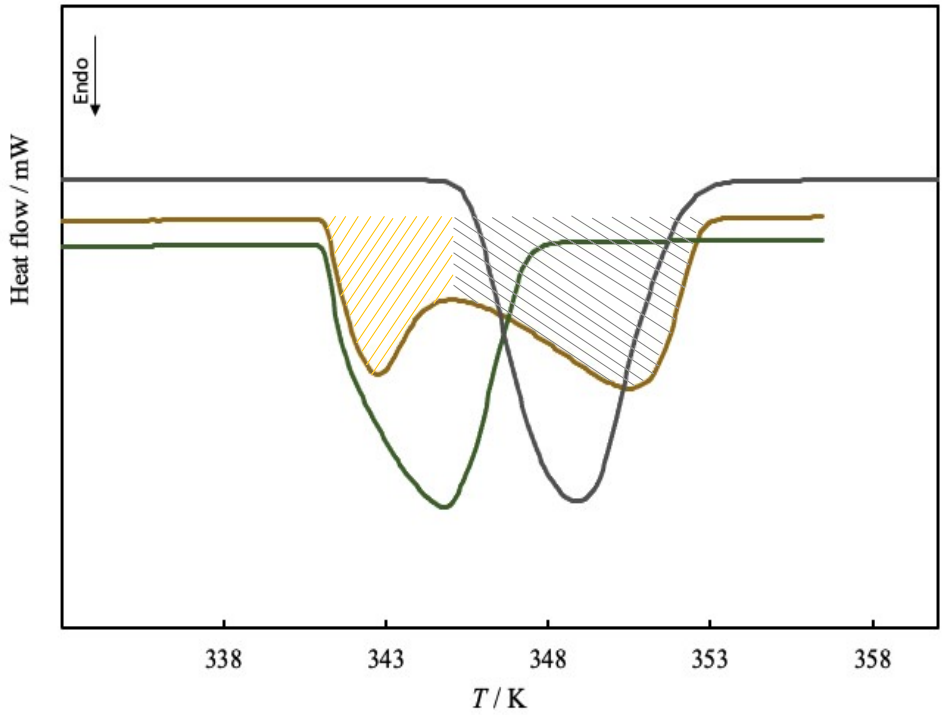

Figure SI.6. – Detailed thermogram for the chloride choline (ChCl) and ChCl + H_2O mixtures at the following compositions: — ChCl, — x_{ChCl} = 0.9, — x_{ChCl} = 0.8.

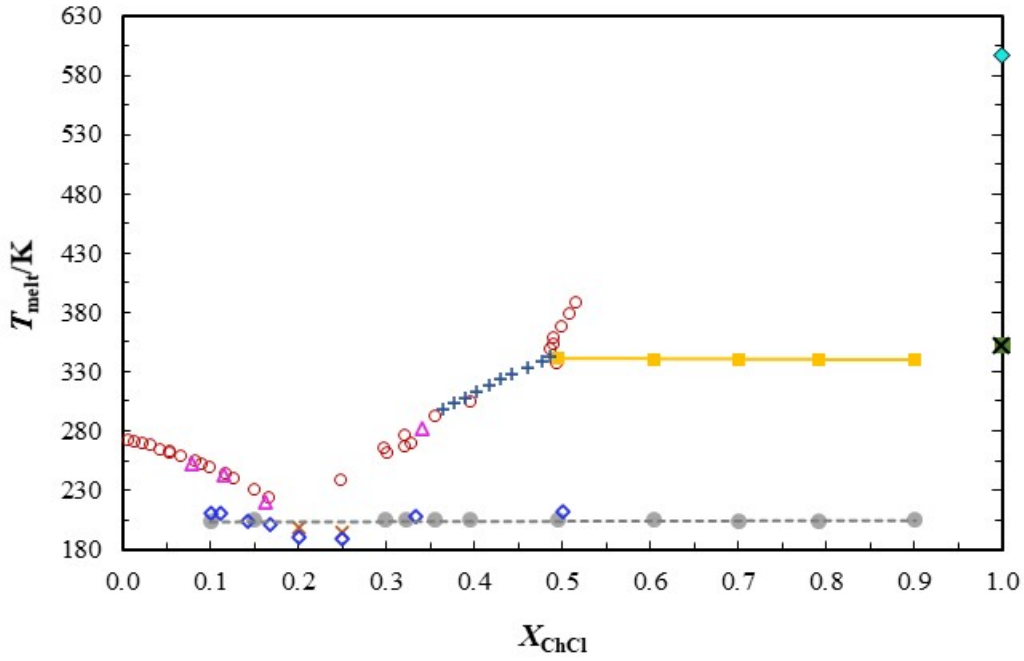

Figure SI.7. Overview of the available solid-liquid equilibrium data for the binary system chlorine chloride and water: from this work, – procedures 1-3; ■ – solid–solid transition of binary ChCl + H_2O mixtures; ■ – solid–solid transition of ChCl; ● – eutectic transition; - Vilas-Boas et al.;[10] - Zhang et al.;[11] - Petrouleas and Lemmon (solid-solid transition of ChCl);[12] - Fernandez et al. (melting of ChCl, estimated);[13] - Asare (eutectic transition);[14] - Rahman and Raynie (eutectic transition).[15]

S7 Calculation of the activity coefficients

The solubility of a solid compound (i) in a liquid, under some assumptions, can be described by:[16]

$$\ln\left(x_i \cdot \gamma_i\right) = \frac{\Delta_m H_i}{R} \cdot \left(\frac{1}{T_{m,i}} - \frac{1}{T}\right) + \frac{\Delta_m Cp_i}{R} \cdot \left(\frac{T_{m,i}}{T} - ln\frac{T_{m,i}}{T} - 1\right) \quad \text{(S1)}$$

in which x and γ are the mole fraction and the activity coefficient of component i in the liquid phase, respectively, $\Delta_m H$ is the melting enthalpy, T_m its melting point, $\Delta_m C_p$ its heat capacity change upon fusion, T is the absolute temperature, and R is the ideal gas constant. Since the heat capacity change upon melting is often unavailable and has a negligible impact on the equilibrium calculations, the heat capacity term in Eq. (S1) can be neglected, resulting in a simpler expression that allow the calculation of the experimental activity coefficient from solid-liquid equilibrium data:

$$\gamma_i = \frac{1}{x_i} exp\left[\frac{\Delta_m H_i}{R} \cdot \left(\frac{1}{T_{m,i}} - \frac{1}{T}\right)\right] \quad \text{(S2)}$$

COSMO-RS

The COnductor like Screening MOdel for Real Solvents (COSMO-RS) is a statistical thermodynamics-based model that predicts the chemical potential of individual components in a mixture.[17,18] To do so, it takes as input the so-called σ-profile of each component and, through pair-wise screened charge contacts, estimates their overall intermolecular interactions. The COSMOtherm software package (BP_TZVP_18 parametrization),[19,20] which is a direct implementation of COSMO-RS, was used in this work to estimate the activity coefficients of water and choline chloride at different compositions. The σ-profile of water was taken from the software database while that of choline chloride was obtained using TURBOMOLE,[21] with a def-TZVP basis set, a BP-86 DFT functional, and the COSMO solvation model (infinite permittivity). In this context, choline chloride was treated as a neutral ionic pair with a conformation akin to that used in previous works.[10,22]

References

1 R. Sabbah, A. Xu-wu, J. S. Chickos, M. L. P. Leitão, M. V. Roux and L. A. Torres, Reference materials for calorimetry and differential thermal analysis, *Thermochim. Acta*, 1999, **331**, 93–204.

2 L. M. N. B. F. Santos, M. A. A. Rocha, A. S. M. C. Rodrigues, V. Štejfa, M. Fulem and M. Bastos, Reassembling and testing of a high-precision heat capacity drop calorimeter. Heat capacity of some polyphenyls at T = 298.15 K, *J. Chem. Thermodyn.*, 2011, **43**, 1818–1823.

3 M. A. A. Rocha, M. Bastos, J. A. P. Coutinho and L. M. N. B. F. Santos, Heat capacities at 298.15 K of the extended [CnC1im][Ntf2] ionic liquid series, *J. Chem. Thermodyn.*, 2012, **53**, 140–143.

4 M. A. A. Rocha, J. A. P. Coutinho and L. M. N. B. F. Santos, Evidence of nanostructuration from the heat capacities of the 1,3-dialkylimidazolium bis(trifluoromethylsulfonyl)imide ionic liquid series, *J. Chem. Phys.*

5 R. D. Chirico, V. Diky, J. W. Magee, M. Frenkel and K. N. Marsh, Thermodynamic and thermophysical properties of the reference ionic liquid: 1-Hexyl-3-methylimidazolium bis[(Trifluoromethyl)Sulfonyl]amide (Including Mixtures). part 2.critical evaluation and recommended property values (IUPAC Technical Report), *Pure Appl. Chem.*, 2009, **81**, 791–828.

6 P. B. P. Serra, F. M. S. Ribeiro, M. A. A. Rocha, M. Fulem, K. Růžička and L. M. N. B. F. Santos, Phase behavior and heat capacities of the 1-benzyl-3-methylimidazolium ionic liquids, *J. Chem. Thermodyn.*, 2016, **100**, 124–130.

7 P. B. P. Serra, F. M. S. Ribeiro, M. A. A. Rocha, M. Fulem, K. Růžička, J. A. P. Coutinho and L. M. N. B. F. Santos, Solid-liquid equilibrium and heat capacity trend in the alkylimidazolium PF6 series, *J. Mol. Liq.*, 2017, **248**, 678–687.

8 J. C. S. Costa, C. F. R. A. C. Lima, A. Mendes and L. M. N. B. F. Santos, Fluorination effect on the thermodynamic properties of long-chain hydrocarbons and alcohols, *J. Chem. Thermodyn.*, 2016, **102**, 378–385.

9 A. S. M. C. Rodrigues, H. F. D. Almeida, M. G. Freire, J. A. Lopes-da-Silva, J. A. P. Coutinho and L. M. N. B. F. Santos, The effect of n vs. iso isomerization on the thermophysical properties of aromatic and non-aromatic ionic liquids, *Fluid Phase*

Equilib., 2016, **423**, 190–202.

10 S. M. Vilas-boas, D. O. Abranches, E. A. Crespo, O. Ferreira, J. A. P. Coutinho and S. P. Pinho, Experimental solubility and density studies on aqueous solutions of quaternary ammonium halides , and thermodynamic modelling for melting enthalpy estimations, *J. Mol. Liq.*, 2020, **300**, 112281.

11 H. Zhang, M. L. Ferrer, M. J. Roldán-Ruiz, R. J. Jiménez-Riobóo, M. C. Gutiérrez and F. Del Monte, Brillouin Spectroscopy as a suitable technique for the determination of the eutectic composition in mixtures of choline chloride and water, *J. Phys. Chem. B*, 2020, **124**, 4002–4009.

12 V. Petrouleas, R. M. Lemmon and A. Christensen, X-ray diffraction study of choline chloride's β form, *J. Chem. Phys.*, 1978, **68**, 2243–2246.

13 L. Fernandez, L. P. Silva, M. A. R. Martins, O. Ferreira, J. Ortega, S. P. Pinho and J. A. P. Coutinho, Indirect assessment of the fusion properties of choline chloride from solid-liquid equilibria data, *Fluid Phase Equilib.*, 2017, **448**, 9–14.

14 S. Asare, Synthesis, characterization and molecular dynamic simulations of aqueous choline chloride deep eutectic solvents, Chemistry and Biochemistry Department, South Dakota State Universty, 2018.

15 M. S. Rahman and D. E. Raynie, Thermal behavior, solvatochromic parameters, and metal halide solvation of the novel water-based deep eutectic solvents, *J. Mol. Liq.*, 2021, **324**, 114779.

16 J. M. Prausnitz, R. N. Lichtenthaler and E. G. de Azevedo, *Molecular thermodynamics of fluid-phase equilibria*, Pretnice Hall PTR, 1999, vol. 3.

17 A. Klamt, Conductor-like screening model for real solvents: A new approach to the quantitative calculation of solvation phenomena, *J. Phys. Chem.*, 1995, **99**, 2224–2235.

18 A. Klamt, V. Jonas, T. Bürger and J. C. W. Lohrenz, Refinement and parametrization of COSMO-RS, *J. Phys. Chem. A*, 1998, **102**, 5074–5085.

19 COSMOtherm, C3.0 Release 2018, COSMOlogic GmbH & Co KG, avaliable on http://www.cosmologic.de.

20 F. Eckert and A. Klamt, Fast solvent screening via quantum chemistry: COSMO-RS approach, *AIChE J.*, 2002, **48**, 369–385.

21 TURBOMOLE V7.1 2016, a development of University of Karlsruhe and

Forschungszentrum Karlsruhe GmbH, 1989-2007, TURBOMOLE GmbH, since 2007, available on http://www.turbomole.com.

22 D. O. Abranches, M. Larriba, L. P. Silva, M. Melle-Franco, J. F. Palomar, S. P. Pinho and J. A. P. Coutinho, Using COSMO-RS to design choline chloride pharmaceutical eutectic solvents, *Fluid Phase Equilib.*, 2019, **497**, 71–78.